Efficient Multi-Scale Halo Artifact Reduction in Chromatic Adaptation Methods for Color Blindness

SIBGRAPI Paper ID: 99999

***Abstract*—Color blindness affects a significant portion of the population, it impacts the visual experience of affected individuals, making chromatic adaptation in digital content crucial for visual accessibility. Existing chromatic adaptation methods effectively improve visual perception but suffer from high computational costs and can produce unwanted halo artifacts. This paper proposes an efficient chromatic adaptation algorithm based on a multi-scale Gaussian pyramid strategy combined with local anisotropic diffusion, effectively eliminating halo artifacts while preserving image quality. Experimental results evaluated with PSNR, local SSIM, MSE, CIEDE2000 and Absolute Difference Maps demonstrate that the proposed method achieves visual quality comparable to state-of-the-art algorithms while drastically reducing processing times by over 90%. Thus, the proposed approach provides an efficient solution, enabling practical real-time applications to enhance visual accessibility for colorblind users.**

I. Introduction

Color blindness is a visual disorder caused by deficiencies in cone cells that detect primary colors. It affects around 8% of men and 0.5% of women globally, limiting their ability to distinguish certain colors [1, 2]. Common types include protanomaly, deuteranomaly, and tritanomaly, which impair the perception of red, green, and blue hues, respectively [3], as shown in Figure 1. These impairments create difficulties in everyday tasks, particularly in digital environments where color distinctions are essential for interpreting content.

To improve accessibility for colorblind users, researchers have developed various chromatic adaptation techniques. Some approaches adjust hues in the HSV space to enhance contrast [4], while others apply recoloring schemes or multiscale strategies tailored to specific deficiencies [5, 6]. Despite their effectiveness, these solutions have notable drawbacks. For instance, Farup's method [7], produces high-quality results with minimal halo artifacts, however is computationally expensive and unsuitable for real-time use. Lighter methods often degrade visual quality by introducing artifacts that reduce clarity and usability.

This study aims to mitigate these limitations by proposing a chromatic adaptation algorithm that strikes a balance between visual quality and computational efficiency. The method integrates a multiscale Gaussian pyramid approach with anisotropic diffusion guided by structure tensors. This combination allows targeted correction in regions prone to halo artifacts, significantly reducing processing time while preserving detail and contrast. Experimental results confirm that the proposed algorithm matches the visual output of state-of-the-art methods but with lower computational costs. This advancement supports the development of real-time tools for enhancing digital accessibility for individuals with color vision deficiencies. In summary, our contributions are: **i)** A multi-scale chromatic adaptation method that combines Gaussian pyramids with anisotropic diffusion to effectively reduce halo artifacts while preserving structural details, enhancing visual accessibility for colorblind users. **ii)** A substantial reduction in computational time—over 90% faster than Farup's original method—while maintaining comparable visual quality.

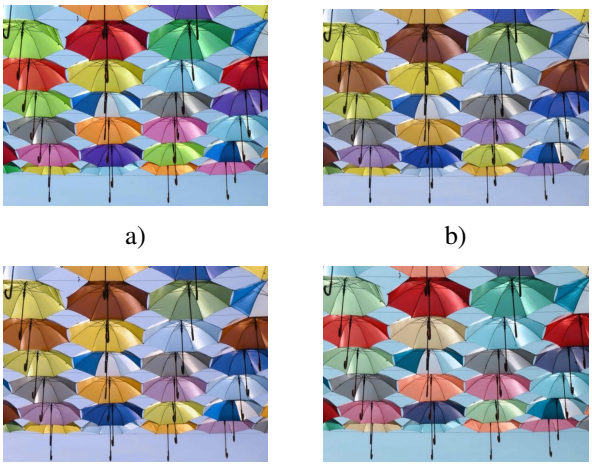

a) b) c) d)

Fig. 1: Example of colorblindness: a) normal vision, b) protanomaly vision, c) deuteranomaly vision, d) tritanomaly vision.

II. Related work

A. Chromatic Adaptation for Color Vision Deficiencies

Several chromatic adaptation methods enhance visual perception for users with color vision deficiencies. Many of these operate directly in the RGB color space due to its suitability for image-level processing. The algorithm presented by Ebelin et al. [8] performs real-time correction by separating luminance and chrominance components. It projects colors onto a dichromatic visibility line and applies weighted histogram equalization, ensuring temporal stability and luminance preservation.

Farup [7] introduced an iterative correction approach based on an optimized color-domain initialization (u_s) which accelerates convergence. This method reconstructs the image from a modified gradient field using local linear anisotropic diffusion. This process effectively reduces halo artifacts near strong chromatic transitions while preserving textures and structural details.

Other color spaces have also been used, although they are less relevant to this work. HSV-based methods [4] modify hue values to enhance contrast for red-green deficiencies. LAB-based corrections, as seen in Elrefaei, Lamiaa's research [3], adjust color components to improve visibility, especially for deuteranopia, and are validated through user studies. LMS approaches [9, 10], simulate cone response to apply biologically motivated adjustments. These focus on salient regions to boost perceived depth and object separation. The HSL-based CBFS method [11] allows personalized chromatic adjustments based on individual needs. Despite these alternatives, RGB remains the preferred space in this research for its balance between simplicity and practical performance.

B. Halo Artifact Reduction in Chromatic Adaptation

Halo artifacts, visible as unwanted bright or dark edges near color transitions, reduce the effectiveness of chromatic adaptation. Minimizing these artifacts is crucial for preserving detail and enhancing perception for colorblind users.

The method presented by Farup [7] addresses this issue with a structure-aware diffusion approach. Traditional isotropic diffusion methods blur edges and often introduce halos. In contrast, the proposed anisotropic diffusion is guided by a structure tensor that maintains edge integrity while smoothing chromatic changes. This reduces halos without compromising image sharpness.

In related domains, dehazing techniques have also addressed halo artifacts. The Bui, Minh-Trung and Kim, Wonha work [12] uses a color ellipsoid model in RGB space to enhance contrast while avoiding halos. It replaces conventional priors with fuzzy segmentation to ensure coherent pixel grouping, especially in heterogeneous regions. Experimental results demonstrate strong performance under dense haze conditions. The strategy presented by Ehsan, Syed et al. [13] introduces dual transmission maps with gradient-domain filtering to suppress halos. It balances local detail preservation and global clarity, producing visually consistent outputs in a range of scenes. Neural networks also contribute to artifact suppression. NAFNet method [14] employs a streamlined architecture without nonlinear activations, focusing on controlled diffusion to preserve fine structures. Though not designed specifically for halo removal, its low-distortion output shows promise. Restormer method [15], a Transformer-based model, combines local and global features through hierarchical layers. It performs well in denoising and motion deblurring, reducing artifacts caused by global transformations. These works offer diverse strategies to reduce halo artifacts. Their contributions inform improvements in chromatic adaptation and broader image enhancement tasks.

III. Theoretical Background

Farup's method [7] serves as the foundation for the present work due to its effectiveness in gradient-domain color correction for individuals with color vision deficiencies (CVD). The algorithm begins by projecting the original RGB image u_0 into a simulated CVD perceptual space using the Brettel model [16]. This step produces a simulated image $s(u_0)$ and its gradient $\nabla s(u_0)$, which are used to assess the loss of chromatic information.

To identify color details lost during the simulation, the algorithm computes a chromatic error image $d_0 = u_0 - s(u_0)$. Principal Component Analysis (PCA) is then applied to extract the dominant direction of chromatic loss, denoted as e_d. To enhance visibility, the algorithm determines an optimal correction direction $e_c = e_d \times e_l$, where e_l represents the luminance direction. Using this, the original gradient ∇u_0 is adjusted to produce a corrected gradient field $G = \nabla u_0 + \chi(\nabla u_0 \cdot e_d)e_c$. The scalar χ controls the intensity of the correction based on both the severity of the CVD and local image characteristics. The corrected image u is reconstructed by solving the Poisson equation $\nabla^2 u - \nabla \cdot G = 0$ through an iterative gradient descent process until convergence is achieved.

To address halo artifacts—commonly introduced during reintegration—the algorithm incorporates anisotropic diffusion. This process is guided by local image structures and defined by the equation $\frac{\partial u}{\partial t} = \nabla \cdot (D \cdot \nabla u)$, where the diffusion tensor D is defined as $D = g(|\nabla u|)I$. The function g, dependent on the gradient magnitude, modulates the diffusion rate, allowing higher diffusion in smooth regions and restricting it near edges to preserve sharp transitions.

The full reintegration process iteratively adjusts the corrected gradient field G, computes the diffusion tensor D from local image gradients, and solves the anisotropic diffusion equation. This iterative approach suppresses halo artifacts while maintaining structural fidelity and enhancing the overall visual quality for color-deficient viewers.

IV. Approach

In this section, a computational method is presented for optimizing the halo artifact minimization algorithm in chromatic adaptation for digital devices designed for colorblind individuals. This method is based on the original proposal by Farup [7], while maintaining the visual quality of the output. The present approach seeks to enhance the user's visual experience by reducing halo artifacts through a multigrid pyramid-based strategy.

The multigrid pyramid-based approach accelerates computation processing while preserving image quality. This approach will be validated using the Peak Signal-to-Noise Ratio (PSNR), Local Structural Similarity Index (Local SSIM), Mean Squared Error (MSE), CIEDE2000 and Absolute Difference Maps metrics to demonstrate that the obtained results do not significantly differ from the original algorithm in terms of visual quality, while achieving improvements in computational cost and processing time.

The color correction algorithm proposed by Farup [7] serves as the foundation for the approach proposed in this paper. This method enhances color perception for individuals with color blindness by minimizing halo artifacts through local linear anisotropic diffusions. While it significantly improves the visual quality of processed images, it has limitations in computation time and residual artifacts near high-contrast

chromatic edges. To overcome these challenges, the proposed method introduces an optimized version leveraging Gaussian pyramids for multiscale processing. This technique enables efficient image correction across multiple resolution levels, reducing computational cost while preserving details and enhancing chromatic adaptation.

The proposed improvement optimizes the anisotropic diffusion process by introducing a multi-scale strategy based on Gaussian pyramids. Instead of applying the correction directly to the full-resolution image, the method decomposes the image into a hierarchy of progressively smaller and smoothed versions. This allows perceptual corrections, such as color adaptation and halo removal, to begin at low resolutions and then be refined as the image is reconstructed at higher levels.

The used Gaussian pyramid is a sequence of images $I_0, I_1, \ldots, I_L$, where I_0 is the original image. $I_{l+1} = G_\sigma * \downarrow (I_l)$, where G_σ is a Gaussian filter with standard deviation σ, and $\downarrow$ denotes downsampling ($\sigma = 1$, image is downsampled by a half). At the coarsest level I_L, where global structures and low-frequency color patterns dominate, anisotropic daltonization is applied. This correction step is modeled by the anisotropic diffusion Partial Differential Equation (PDE):

$$\frac{\partial u}{\partial t} = \nabla \cdot (D \nabla u), \tag{1}$$

where $u(x, y, t)$ is the image evolving, and D is the diffusion tensor that controls the direction and intensity of diffusion based on local gradients and structures. This diffusion process is computed only at level I_L, reducing computational cost while capturing broad perceptual adjustments.

The corrected image is then reconstructed through a coarse-to-fine cycle. At each level l, the solution from level $l + 1$ is upsampled using bilinear interpolation and refined by adding a high-frequency residual:

$$u_l = \mathcal{P}(u_{l+1}) + \Delta u_l, \tag{2}$$

where $\mathcal{P}(u_{l+1})$ denotes the upsampled result from the coarser level, and Δu_l is the correction term obtained as the difference between the original image at level l and the downsampled version of the upsampled output. This ensures that fine details are progressively recovered while preserving the structural and perceptual modifications introduced at the coarse scale.

This multigrid approach offers several advantages. One key benefit is the improved halo reduction, achieved by smoothing chromatic transitions at coarser levels, which effectively suppresses halo artifacts early in the process and prevents their propagation to finer levels. Additionally, the method ensures edge preservation, as the diffusion tensor is recomputed at each scale, maintaining the sharpness of important edges throughout the correction. In terms of performance, the strategy enhances computational efficiency, as processing at low resolutions reduces both the number of pixels involved and the computational workload. At the same time, high-resolution levels require only localized refinements. Finally, the method guarantees spatial consistency, as local neighborhood operations are preserved across all scales, ensuring coherent results without relying on highly parallel or synchronization-sensitive algorithms.

V. Experiments

To validate the proposed chromatic correction method, we apply both quantitative metrics and user-based evaluations. In addition to MSE and PSNR, we introduce local SSIM to measure structural similarity at a finer spatial scale. This highlights localized artifacts that global SSIM may overlook. We also compute CIEDE2000, which quantifies perceptual color differences and is well-suited for assessing changes relevant to color vision deficiencies (CVD).

Absolute difference maps are generated to visualize pixel-wise corrections and halo reduction. We supplement these metrics with qualitative visual comparisons, showing side-by-side examples of corrected and uncorrected images. These illustrate improvements in chromatic clarity, edge preservation, and artifact suppression. A user study with CVD participants measures practical gains in numerical pattern recognition, reinforcing the method's real-world impact.

A. Dataset

For our experiments we followed the test protocol proposed by Farup [7], which consists of photographs with dominant red-green and blue-yellow contrasts, as shown in Figure 2.

The evaluation of the obtained results will focus on interpreting the values of the applied metrics to assess visual quality, structural similarity, and perceptual color differences. In particular, PSNR values above 30 dB indicate high visual quality, whereas values below 20 dB suggest noticeable degradation. SSIM values close to 1 reflect strong structural similarity between the original and processed images. The use of local SSIM enables fine-grained analysis, helping to detect localized artifacts or detail loss that the global score may not capture. Low MSE values indicate minimal pixel-wise differences, reinforcing the accuracy of the processed image concerning the reference.

To assess perceptual color consistency—especially relevant for color vision deficiencies (CVD)—the CIEDE2000 metric is employed. Lower CIEDE2000 values imply better perceptual color alignment, and in the context of CVD, they help validate whether color transformations are non-intrusive. Absolute difference maps are also used as visual aids to highlight regions where improvements occur, such as halo reduction or enhanced edge clarity.

Together, these metrics provide both objective and perceptual evidence of the effectiveness of the proposed optimization. The results will demonstrate that the quality of the processed images remains comparable to, or improves upon, that of the original algorithm [7], validating the approach as a viable and competitive alternative.

B. Results and discussion by evaluation metric

i) User Testing To validate the effectiveness of the proposed method while preserving visual quality, a user evaluation was conducted with six colorblind participants. Each individual had

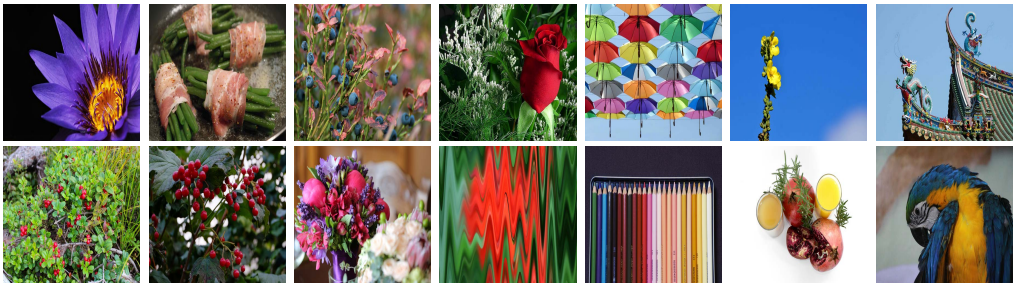

Fig. 2: Image dataset proposed by Farup [7].

previously diagnosed their type and severity of color vision deficiency using the Ishihara test [17], which served to inform the initial settings for the chromatic correction process. Among the participants, 5 exhibited deuteranomaly (green-weakness), and 1 presented protanomaly (red-weakness). All subjects were shown a total of 37 standard Ishihara plates in their original form and were asked to identify the numbers embedded in each. If no number could be perceived, participants explicitly indicated the absence of a discernible figure.

Regarding the results with the original, uncorrected images, participants correctly identified an average of 12.94 out of 37 plates. These figures highlight the significant difficulty color-blind individuals face when attempting to perceive numerical information without chromatic correction.

Following the application of the proposed correction method, the same evaluation was repeated. In this second round, all participants were able to correctly identify all 37 plates. This outcome demonstrates a notable improvement in visual clarity and numeric recognition, confirming the effectiveness of the method in enhancing color discrimination and mitigating the perceptual limitations associated with color vision deficiency.

ii) Execution Time Although the method presented by Farup effectively reduces halo artifacts, it entails a high computational cost, resulting in longer processing times. In contrast, the proposed approach achieves comparable visual results with significantly enhanced computational efficiency.

To quantify this improvement, the average execution time was computed over 10 runs for both the original algorithm from [7] and the proposed method, using each image in the dataset. The comparative results are summarized in Table I.

The optimized algorithm reduces execution time by over 90%, dropping from an average of 24.57 s - 36.34 s per image to 2.06 s - 2.90 s. This demonstrates a substantial improvement in processing efficiency.

Across all images, execution times consistently improve. For instance, Image 1 reduced from 24.72 s to 2.06 s, becoming 91.7% faster, and Image 5 decreased from 36.34 s to 2.90 s. The use of Gaussian pyramids plays a key role, as it reduces processing time by operating on lower-resolution levels first, minimizing computational requirements during the halo reduction phase.

iii) Local SSIM, MSE, and PSNR A quantitative comparison was conducted using three established image quality metrics:

TABLE I: Comparison of execution times between the original algorithm presented by Farup [7] and the proposed algorithm.

	Execution Time (s)	
Image	**Farup [7]**	**Ours**
Img 1	24.72	2.06
Img 2	24.57	2.12
Img 3	29.21	2.37
Img 4	33.84	2.78
Img 5	36.34	2.90
Img 6	30.23	2.54
Img 7	31.19	2.49
Img 8	30.24	2.49
Img 9	30.23	2.56
Img 10	29.24	2.54
Img 11	29.26	2.55
Img 12	29.37	2.48
Img 13	29.01	2.42
Img 14	29.22	2.42
μ/σ	29.96 ± 2.94	**2.50 ± 0.22**
Total	478.11	**34.63**

Local Structural Similarity Index (Local SSIM), Peak Signal-to-Noise Ratio (PSNR), and Mean Squared Error (MSE). These metrics were selected to evaluate structural preservation, visual fidelity, and pixel-wise error, respectively.

Table II and Figure 3 present a comparative analysis between the original method, the proposed approach, and several state-of-the-art techniques from related fields such as halo reduction, denoising, and deblurring [12–15]. Although these methods were originally developed for different purposes, they share the common goal of suppressing halo artifacts. Figure 3 specifically illustrates an example of Local SSIM values, emphasizing the subtle improvements introduced by the proposed method over the original implementation.

The results demonstrate that the proposed method achieves performance comparable to that of the original algorithm developed by Farup. A direct comparison of the images generated by both approaches revealed high structural similarity and minimal reconstruction error. In contrast, alternative methods such as those described in [12–15] exhibited reduced effectiveness in this specific context, as summarized in Table II. These findings confirm that the proposed method successfully preserves visual quality while offering a competitive alternative

to existing state-of-the-art techniques.

TABLE II: Comparison of metrics between the proposed method and other halo reduction approaches.

Method	SSIM	PSNR (dB)	MSE
Kim et.al[12]	0.80	28.89	91.53
Ehsan et.al[13]	0.87	18.15	87.21
Chen et.al[14]	0.70	10.40	0.10
Real Denoising[15]	0.73	10.20	0.11
Motion Deblurring[15]	0.73	10.07	0.11
Proposed	**0.9981**	**37.93**	**0.0002**

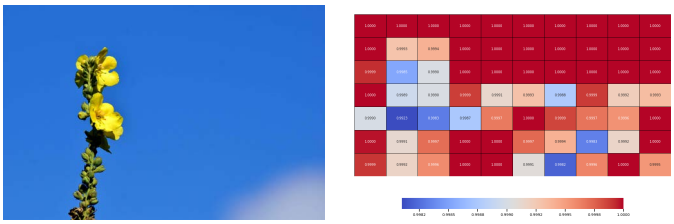

Fig. 3: Local SSIM matrix comparing our proposed method with Farup's method.

As further evidence of this quality improvement, we include a direct comparison between the proposal and the original algorithm by Farup, both evaluated against the uncorrected images. PSNR was used as the reference metric to assess how closely each corrected image approximates the original input. The proposed method consistently achieved higher PSNR values, exceeding the original method on drastically changing color zones. As shown in Figure 4.

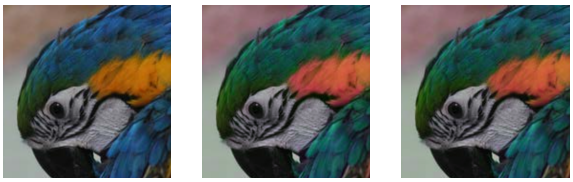

Fig. 4: Visual comparison between the original image, Farup's method [7], and the proposed method. PSNR: 25.85 dB. PSNR (Original vs. Proposed): **27.32 dB**.

iv) CIEDE 2000 To evaluate the perceptual differences introduced by the chromatic adaptation process, the CIEDE2000 color difference (ΔE_{00}) was calculated between the original and corrected images from the dataset described in Figure 2, using the CIE Lab color space. Each image was segmented into non-overlapping 20×20 pixel windows, and the average ΔE_{00} was computed within each window.

This methodology enables a localized analysis of chromatic variation, offering results that better align with human visual perception. Regions exhibiting high values, specifically where $\Delta E_{00} > 5$, correspond to areas where the color correction had the most significant perceptual impact. Conversely, low ΔE_{00} values suggest minimal perceptual alteration. The distribution of these values confirms that the proposed method performs targeted chromatic adaptation, focusing on areas of high perceptual ambiguity that are particularly challenging for individuals with color vision deficiency, instead of applying uniform corrections across the entire image.

As shown in Figure 5.a, the boxplot compares the ΔE_{00} values obtained with the proposed method and the LMS Daltonization algorithm [3]. Figures 5.g and 5.h present the ΔE_{00} matrices resulting from the comparisons between the original image and the output of the proposed method, and between the original image and the LMS Daltonization output, respectively. These results demonstrate that the proposed color correction approach performs selective, context-aware adaptations, in contrast to the global adjustments applied by other algorithms, like LMS Daltonization. The mean ΔE_{00} values range from 2.5 to 14.7 across the dataset, reflecting perceptible yet spatially localized differences. The standard deviation values further confirm that the corrections are concentrated in regions with higher chromatic ambiguity, thereby enhancing perceptual clarity where it is most needed while preserving the overall structure of the image.

v) Absolute Difference Maps To visually support the effectiveness of the proposed method in suppressing halo artifacts while preserving edge structures, absolute difference maps $|I_1 - I_2|$ were employed. Figures 5.e and 5.f show the outputs of the proposed method and Farup's algorithm, respectively. Figure 5.i displays the absolute difference map $(I_F - I_P)$, dark areas dominate, indicating that most changes are subtle and localized. This behavior implies a more precise halo correction that avoids unnecessary modifications in uniform regions. The results confirm that the proposed method produces minimal deviations from Farup's approach, preserving visual fidelity.

VI. Conclusions

The proposed method shows as a suitable alternative for color correction and halo reduction implementations. It preserves visual quality, with an average PSNR of 37.93 dB, local SSIM of 0.9981, and MSE of 0.0002. CIEDE2000 results showed that chromatic adjustments were concentrated in perceptually relevant regions without altering uniform areas. Absolute difference maps confirmed that changes were focused on sensitive edges, avoiding unnecessary global modifications. User testing revealed complete improvement in numerical pattern recognition after applying the correction. Compared to the original method by Farup, the proposed method achieved improved results, while other halo reduction techniques showed lower performance in this context.

References

[1] P. Doliotis, G. Tsekouras, C.-N. Anagnostopoulos, and V. Athitsos, "Intelligent modification of colors in digitized paintings for enhancing the visual perception of color-blind viewers," vol. 296, 04 2009, pp. 293–301.

[2] J. Choi, J. Lee, H. Moon, S. J. Yoo, and D. Han, "Optimal color correction based on image analysis for color vision deficiency," *IEEE Access*, vol. 7, pp. 154 466–154 479, 2019.

[3] L. Elrefaei, "Smartphone based image color correction for color blindness," *International Journal of Interactive Mobile Technologies (iJIM)*, vol. 12, p. 104, 07 2018.

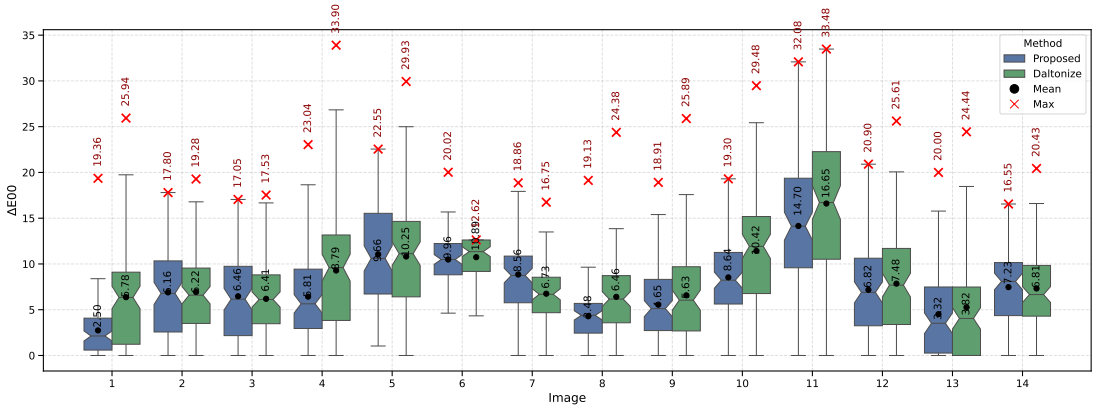

a)

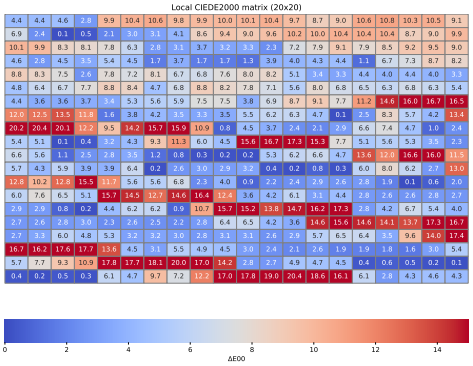

(g)

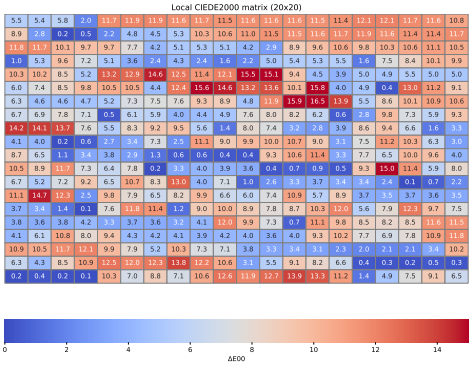

(h)

(b)

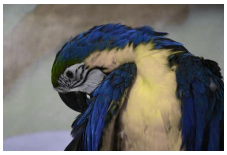

(c)

(d)

(e)

(f)

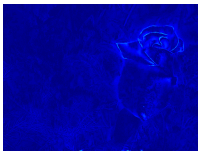

(i)

Fig. 5: Visual and quantitative evaluation. **a)** Boxplot of CIEDE2000 differences comparing the proposed method and LMS Daltonization. **b)**original image. **c)**LMS Daltonization output, **d)**proposal output for ΔE_{00} experiment, **e)** proposal output for absolute different maps experiment, **f)**Farup's method output, **g)-h)**local ΔE_{00} matrix of proposed and LMS Daltonization methods, **i)**absolute difference map $(I_F - I_P)$ between Figures **e** and **f**.

[4] K. Erdogan and N. Yilmaz, "Shifting colors to overcome not realizing objects problem due to color vision deficiency," in *2nd Int. Conf. on Advances in Computing, Electronics and Electrical Technology-CEET*, 2014, pp. 11–14.

[5] M. Ribeiro and A. J. P. Gomes, "Recoloring algorithms for colorblind people: A survey," *ACM Comput. Surv.*, vol. 52, no. 4, aug 2019.

[6] J. T. Simon-Liedtke and I. Farup, "Multiscale daltonization in the gradient domain," *Journal of Perceptual Imaging*, vol. 1, no. 1, pp. 10 503–1, 2018.

[7] I. Farup, "Individualised halo-free gradient-domain colour image daltonisation," *Journal of Imaging*, vol. 6, 2020.

[8] G. D. M. O. K. T. A.-M. P. Ebelin, C. Crassin, "Luminance-preserving and temporally stable daltonization — research," *Nvidia Research*, May 2023. [Online]. Available: https://research.nvidia.com/publication/2023-05_daltonization

[9] S. Bighiu, "An investigation towards designing decentralized applications for individuals with visual impairments," *University of Groningen*, 2022.

[10] F. X. . F. H. Li, J., "Saliency-based image correction for colorblind patients." *Computational Visual Media*, vol. 6, jun 2020.

[11] B. Swathi, R. Koushalya, J. Vishal Roshan, and M. Gowtham, "Color blindness algorithm comparison for developing an android application," *International Research Journal of Engineering and Technology (IRJET)*, 2020.

[12] M.-T. Bui and W. Kim, "Single image dehazing using color ellipsoid prior," *IEEE Transactions on Image Processing*, vol. PP, pp. 1–1, 11 2018.

[13] S. Ehsan, M. Imran, A. Ullah, and E. Elbaşı, "A single image dehazing technique using the dual transmission maps strategy and gradient-domain guided image filtering," *IEEE Access*,

vol. PP, pp. 1–1, 06 2021.

[14] L. Chen, X. Chu, X. Zhang, and J. Sun, "Simple baselines for image restoration," 2022. [Online]. Available: https://arxiv.org/abs/2204.04676

[15] S. W. Zamir, A. Arora, S. Khan, M. Hayat, F. S. Khan, and M.-H. Yang, "Restormer: Efficient transformer for high-resolution image restoration," 2022.

[16] H. Brettel, F. Viénot, and J. D. Mollon, "Computerized simulation of color appearance for dichromats," *J. Opt. Soc. Am. A*, vol. 14, no. 10, pp. 2647–2655, Oct 1997.

[17] D. S. Ishihara, *The Series of Plates Designed as a Test for Colour-Blindness 24 Plates Edition*, 1964.